

Eribulin mesylate induces bone mass loss by promoting osteoclastic bone resorption in mice

Takahiro Ishizaka^a, Keisuke Horiuchi^{a,*}, Shinya Kondo^a, Masashi Isaji^a, Takahiro Nakagawa^a, Masahiro Inoue^a, Hajime Rikitake^a, Eiko Taguchi^a, Michiro Susa^a, Masaki Yoda^b, Takeshi Ono^c, Yusuke Kozai^d, Kazuhiro Chiba^a

^a Department of Orthopedic Surgery, National Defense Medical College, Namiki 3-2, Tokorozawa, Saitama 359-8513, Japan

^b Department of Orthopaedic Surgery, Keio University School of Medicine, 35 Shinanomachi, Shinjuku, Tokyo 160-8582, Japan

^c Department of Global Infectious Diseases and Tropical Medicine, National Defense Medical College, Namiki 3-2, Tokorozawa, Saitama 359-8513, Japan

^d Department of Education Planning, Kanagawa Dental University, 82 Inaokacho, Yokosuka, Kanagawa 238-8580, Japan

ARTICLE INFO

Keywords:

Cancer treatment-induced bone loss
Eribulin mesylate
Osteoclast
Bisphosphonate
RANKL
Osteoprotegerin

ABSTRACT

Over the past few decades, the clinical outcomes of patients with cancer have significantly improved mostly owing to the development of effective chemotherapeutic treatments. However, chronic health conditions such as bone mass loss and risk of fragility fractures caused by chemotherapy have also emerged as crucial issues in patients treated for cancer. In this study, we aimed to understand the effect of eribulin mesylate (ERI), a microtubule-targeting agent currently used to treat metastatic breast cancer and certain subtypes of advanced sarcomas, on bone metabolism in mice. The administration of ERI reduced bone mass in mice, mainly by promoting osteoclast activity. Gene expression analysis of skeletal tissues revealed no change in the expression levels of the transcripts for RANK ligand, one of the master regulators of osteoclastogenesis; however, the transcript levels of osteoprotegerin, which neutralizes RANK ligand, were significantly reduced in ERI-treated mice compared with those in vehicle-treated controls, indicating a relative increase in RANK ligand availability after ERI treatment. In line with the increased bone resorption in ERI-treated mice, we found that zoledronate administration effectively suppressed bone loss in these mice. These results reveal a previously unrecognized effect of ERI on bone metabolism and suggest the application of bisphosphonates for patients with cancer undergoing treatment with ERI.

1. Introduction

The clinical outcomes of patients with cancer have improved significantly over the past few decades owing to the development of effective treatments and diagnostic measures. However, as the number of cancer survivors increases, various chronic health conditions, including physical and mental disorders, have emerged as crucial clinical issues (Neo et al., 2017; Couzin-Frankel, 2019). Cancer survivors have been recently found to be at a greater risk of developing osteopenia and osteoporosis among various other health conditions, which could ultimately lead to fragility fractures (Kommalapati et al., 2017; Handforth et al., 2018; Guise, 2006; Kanis et al., 1999; Saad et al., 2008). This condition, also referred to as cancer treatment-induced bone loss (CTIBL), can be attributed to various factors including immobilization due to long-term hospitalization, radiation, malnutrition, and

chemotherapy.

Hitherto, CTIBL has mostly been investigated in patients with breast and prostate cancer who underwent anti-hormonal therapy, such as aromatase inhibitor-based and androgen deprivation therapies (Handforth et al., 2018; Guise, 2006; Saad et al., 2008; Rachner et al., 2018). Given that skeletal homeostasis is highly susceptible to fluctuations in gonadal hormone levels and that anti-hormonal therapy often spans years, it may not be surprising that patients with breast cancer and prostate cancer have been the focus of clinical research on CTIBL. Nonetheless, *in vivo* and *in vitro* studies have shown that cytotoxic chemotherapeutic agents such as epirubicin (Huang et al., 2018), methotrexate (Georgiou et al., 2012; Shandala et al., 2012), doxorubicin (DOX) (Fan et al., 2017; Yao et al., 2020; Rana et al., 2013), cyclophosphamide (Fan et al., 2017), and melphalan (Chai et al., 2017) can induce bone loss through multiple mechanisms that do not involve

* Corresponding author at: Department of Orthopedic Surgery, National Defense Medical College, 3-2 Namiki, Tokorozawa, Saitama 359-8513, Japan.
E-mail address: khoriuchi@ndmc.ac.jp (K. Horiuchi).

hormone deprivation. While it is not yet clear to what extent these cytotoxic agents contribute to CTIBL in cancer survivors, a recent cohort study revealed that older cancer survivors who received chemotherapy had a higher risk of fragility fractures than older adults without cancer (Rees-Punia et al., 2023). The results of this study indicate that chemotherapy has a significant impact on long-term bone health in cancer survivors and underlines the importance of understanding the effects and mechanisms of chemotherapeutic agents on CTIBL.

Eribulin mesylate (ERI) is a microtubule-targeting agent currently used to treat metastatic breast cancer and advanced liposarcoma (Dybdal-Hargreaves et al., 2015; Swami et al., 2012; Mougalian et al., 2021). Although patients with breast cancer (primarily middle-aged and older women) as well as those with liposarcoma (mostly elderly) are likely to face an increased risk of lower bone mass, the potential effect of ERI on long-term bone health conditions remains uninvestigated.

Thus, in the present study, we aimed to elucidate the potential effects of ERI on the bone microstructure and metabolism. We found that the administration of ERI reduced bone mass, mainly by promoting osteoclastic bone resorption. Gene expression analysis of skeletal tissues revealed no change in the expression levels of the transcripts for RANK ligand, a membrane-bound molecule critically involved in the regulation of osteoclastogenesis (Xing et al., 2005); however, the transcript levels of osteoprotegerin (OPG), a decoy receptor of RANK ligand, were significantly reduced in ERI-treated mice compared with the vehicle (VCL)-treated controls, indicating that there was a relative increase in RANK ligand availability after ERI treatment. In accordance with the increased osteoclast activity in ERI-treated mice, we found that a single administration of zoledronate (ZOL), a potent anti-osteoclastic agent, completely prevented bone loss induced by the administration of ERI. Taken together, our data reveal a previously unrecognized effect of ERI on bone metabolism and suggest that patients with cancer who need to be treated with ERI may benefit from the prophylactic administration of bisphosphonates.

2. Materials and methods

2.1. Cell line and agents

The mouse macrophage-like cell line RAW264.7 was obtained from Riken Bioresource Center (Ibaraki, Japan). RAW264.7 cells were cultured in alpha-modified Eagle's minimal essential medium (Sigma-Aldrich, St. Louis, MO) supplemented with 10 % fetal bovine serum, penicillin-streptomycin (100 U/ml), and 1 % non-essential amino acids at 37 °C under 5 % CO₂. ERI, DOX, trabectedin (TBD), and ZOL were purchased from Eisai (Tokyo, Japan), Aspen (Tokyo, Japan), Taiho Pharmaceutical (Tokyo, Japan), and Novartis Pharma (Tokyo, Japan), respectively. All agents were dissolved in phosphate-buffered saline and stored at -20 °C until use. Serum testosterone levels were determined using the Testosterone Parameter Assay Kit KGE010 (R&D Systems, Minneapolis, MN). The antibodies used for flow cytometry were purchased from BioLegend (San Diego, CA).

2.2. Mice

10-week-old C57BL/6N male mice were purchased from Japan SLC (Shizuoka, Japan) and maintained under specific pathogen-free conditions at constant temperature and humidity. Mice were randomized into four groups: VCL-, ERI-, DOX-, and TBD-treated groups. The doses of the chemotherapeutic agents used in the present study were decided based on the protocols of previous studies (Yao et al., 2020; Taguchi et al., 2021; Inoue et al., 2022), as 5 mg/kg, 0.1 mg/kg, and 1 mg/kg for DOX, TBD, and ERI, respectively. The agents were intravenously administered every 7 days for three cycles. One week after the final injection, the mice were euthanized by cervical dislocation, and the serum, lumbar vertebrae, tibiae, and femurs were collected for analysis. In certain experiments, mice were intraperitoneally injected with ZOL (0.1 mg/kg,) once

on the day of the first ERI injection. All animal experiments were approved by the Animal Care Committee of National Defense Medical College (Approval Number:19055).

2.3. Micro-computed tomography (μ CT) analysis

Scanning was performed using a μ CT system (ScanXmate-D090S105) and Xsys software (Comscantecno, Kanagawa, Japan) with a voxel size of 10 μ m. Three-dimensional microstructural image data were reconstructed using ConeCT express software (White Rabbit, Tokyo, Japan), and the structural indices were computed using Analyze 14.0 software (Analyze Direct, Overland Park, KS). The region of interest was set at 200–1200 μ m, distal to the proximal growth plate of the tibia.

2.4. Peripheral quantitative computed tomography analysis

Cross-sections of the proximal and midshaft of the tibia (1.7 and 7.0 mm distal to the proximal growth plate, respectively) were scanned using a Stratec XCT Research SA+ Small Animal QCT system (Stratec Medizintechnik, Pforzheim, Germany) with a tube voltage of 50.4 kV, tube current of 236 μ A, X-ray power of 11.9 W, and voxel size of 80 \times 80 \times 460 μ m. Cut-off values of 267 and 690 mg/cm³ were applied to the trabecular and cortical bone, respectively. Bone mineral density (BMD) values at 1.7 and 7.0 mm distal to the proximal growth plate were defined as trabecular BMD and cortical BMD, respectively.

2.5. Mechanical property analysis

The mechanical properties of the femur were assessed using a three-point bending test with an MZ-500S instrument (Maruto, Tokyo, Japan). The femurs were secured on the two lower supports separated by 6 mm. The bending load was applied at the center of the femoral shaft in the anteroposterior direction at a speed of 10 mm/min. The following mechanical indices were recorded: ultimate force (maximal force supported by the bone before fracture, N), breaking force (work required to fracture the bone, N), and stiffness (extrinsic rigidity of the femur, N/mm).

2.6. Histomorphometric analysis

Mice were subcutaneously injected with 10 mg/kg calcein 5 and 2 days before euthanasia. Lumbar vertebrae were removed and fixed with 70 % ethanol for three days. The fixed specimens were stained with Villanueva bone stain solution for six days, embedded in methyl methacrylate resin, and sectioned at 5 μ m thickness.

2.7. Quantitative PCR

Both ends of the femurs were severed and the bone marrow was removed by centrifugation as previously described (Amend et al., 2016). Bone specimens devoid of bone marrow were homogenized in ISOGEN II RNA Extraction Reagent (Nippon Gene, Tokyo, Japan) using a μ T-12 bead crusher (Taitec, Saitama, Japan) to collect RNA. cDNA was synthesized using the PrimeScript RT Reagent Kit (TaKaRa Bio, Shiga, Japan) as instructed by the manufacturer. Semi-quantitative PCR was performed using TB Green Premix Ex Taq II (TaKaRa Bio) on a ViiA 7 Real-Time PCR System (Life Technologies, Carlsbad, CA). Gene expression levels were normalized to the expression levels of *Gapdh* transcripts. The expression levels of the transcripts of each gene in VCL-treated mice were set to 1. All analyses were performed in duplicate. The nucleotide sequences of the oligonucleotides used in this study are listed in Supplementary Table S1.

2.8. Flow cytometry

Femurs and tibiae were collected one week after ERI or VCL injection. The bone marrow was flushed with RPMI-1640 medium (Sigma-

Aldrich) from the femurs and tibiae and filtered through a cell strainer (70 μ m; BD Falcon, Franklin Lakes, NJ) to remove debris. Mononuclear cells were isolated by centrifugation from total bone marrow cells using Histopaque-1083 (Sigma-Aldrich), following the manufacturer's instructions. Cells were incubated with the following antibodies to detect osteoclast precursors (Arai et al., 1999): FITC-conjugated anti-CD11b (clone M1/70), phycoerythrin-conjugated anti-CD115 (c-Fms; clone AFS98), and APC-conjugated anti-CD117 (c-Kit; clone 2B8). Flow cytometric analysis was performed using a NovoCyte flow cytometer and the NovoExpress software (ACEA Biosciences, San Diego, CA).

2.9. Osteoclast formation and gene expression assay

RAW264.7 cells and primary bone marrow cells were used. Bone marrow cells were harvested from the femurs and tibiae of 8-week-old mice. The cells were cultured with 50 ng/ml recombinant murine M-CSF (Peprotech, Cranbury, NJ) for 3 days on petri dishes. The adherent cells were used as bone marrow macrophages. RAW264.7 cells were plated on 96-well plates at 1×10^4 cells per well in the presence of 100 ng/ml recombinant human soluble RANK ligand (Peprotech) for 6 days. Bone marrow macrophages were plated in 96-well plates at 1.25×10^4

cells per well and further incubated in the presence of 50 ng/ml M-CSF and 100 ng/ml soluble RANKL for 5 days. The cells were exposed to different concentrations of ERI (0, 1, 10, or 50 nM) during incubation. Subsequently, cells were fixed with 4 % paraformaldehyde and stained for tartrate-resistant acid phosphatase (TRAP) using a TRAP Staining Kit (Cosmo Bio, Tokyo, Japan). The number of osteoclasts, defined as TRAP-positive multinucleated cells with more than three nuclei, was counted under a microscope (BZ-X710; Keyence, Osaka, Japan). Nine microscopic fields were randomly evaluated and the total sum was calculated for each specimen. For gene expression analyses, cells were collected 48 h after stimulation with soluble RANK ligand. Semi-quantitative PCR was performed as previously described.

2.10. Statistical analysis

Statistical analyses were performed using one-way analysis of variance followed by Dunnett's post-hoc test for multiple comparisons or two-tailed Student's *t*-test for a comparison of two groups using GraphPad Prism 8 (GraphPad Software, San Diego, CA). Data are expressed as the mean \pm standard error of the mean. *P* values <0.05 were considered statistically significant.

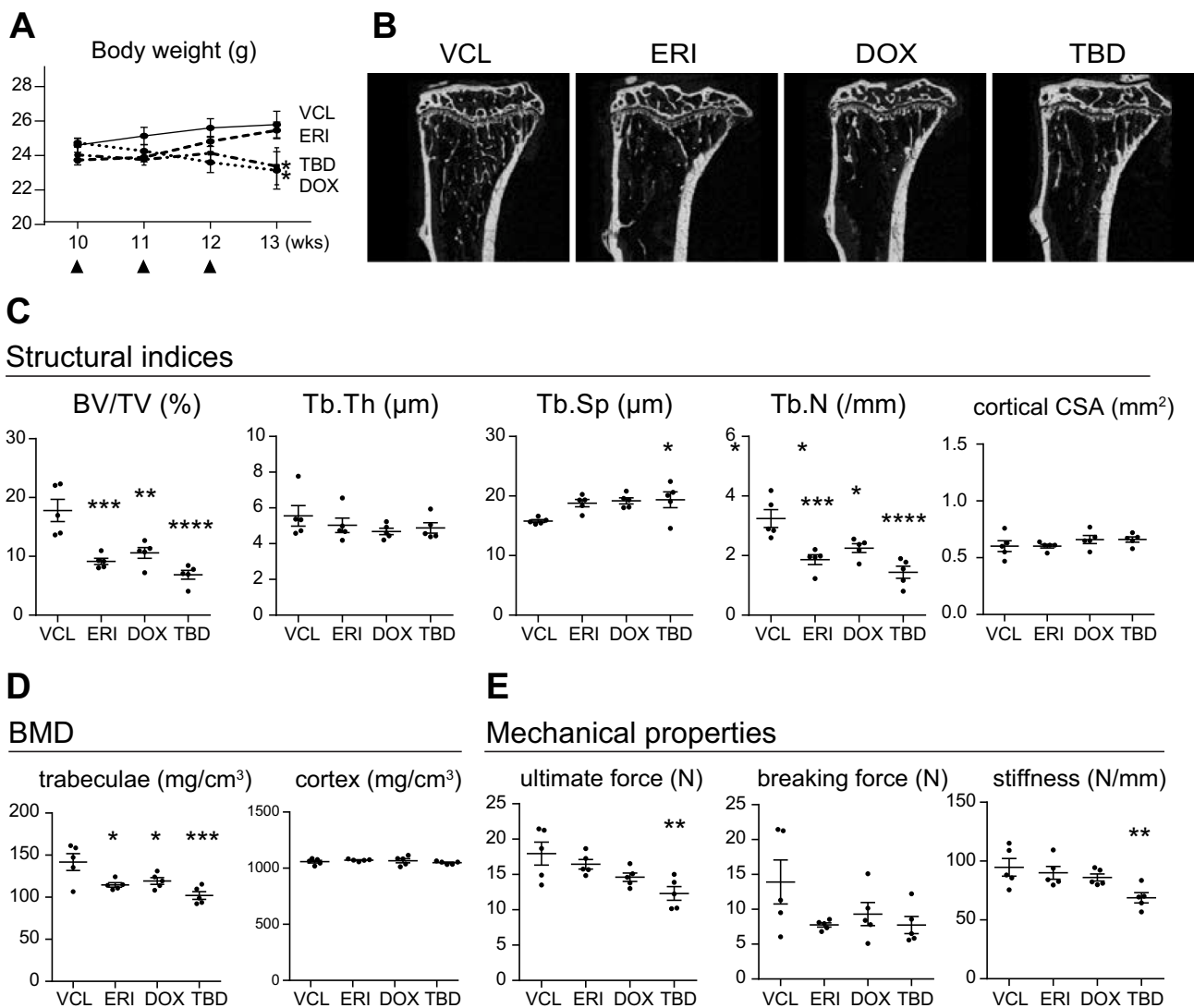


Fig. 1. ERI, DOX, and TBD induce bone mass loss in mice. A. Time-course changes in the body weight of mice in each treatment group. Black arrowheads indicate the administration of chemotherapeutic agents. B. Representative reconstructed μ CT images of the proximal tibia of each treatment group. C, D, and E. Structural indices (C), BMD (D), and mechanical properties (E) of mice in each treatment group. Five mice per each treatment group were analyzed. *, *P* < 0.05; **, *P* < 0.01; ***, *P* < 0.001; ****, *P* < 0.0001 (compared with those in the VCL-treated group).

3. Results

3.1. ERI induces bone mass loss in mice

10-week-old wild-type male mice were intravenously administered either VCL, DOX (5 mg/kg), TBD (0.1 mg/kg), or ERI (1 mg/kg) once a week for three times and euthanized for analysis 4 weeks after the first injection as described in the Materials and Methods. DOX is one of the most widely used chemotherapeutic agents in the treatment of malignant tumors including breast cancer, lymphoma, soft tissue sarcomas, and osteosarcoma. TBD is a novel chemotherapeutic agent that has been approved as a second-line agent for treating liposarcoma and leiomyosarcoma (Demetri et al., 2016). Both DOX and TBD have been shown to induce bone mass loss in mouse models (Fan et al., 2017; Yao et al., 2020; Rana et al., 2013; Sinder et al., 2017) and were included in the present study for comparison. Treatment with DOX and TBD resulted in significant body weight loss at the dose and frequency prescribed in the present study (Fig. 1A). In contrast, body weight loss in ERI-treated mice was markedly lower than that in DOX- or TBD-treated mice.

Structural analysis of the proximal tibia using μ CT revealed that treatment with ERI resulted in comparable levels of bone mass loss in the trabecular bone (decrease in the volume of mineralized bone per unit volume (BV/TV), number of trabeculae per unit volume (Tb/N), and an increase in the space between trabeculae (Tb/Sp) as seen after DOX or

TBD treatment (Fig. 1B and C). The decrease in trabecular BMD was also comparable among all treatment groups (Fig. 1D). In contrast, under the present experimental conditions, there were no changes in trabecular thickness (Tb/Th), cortical cross-sectional area (CSA) of the proximal tibia, or cortical BMD in any of the treatment groups compared with those in the VCL-treated control animals. Analysis of mechanical properties by a three-point bending test showed that the mice of treatment groups had more fragile bones than those in the VCL-treated group; however, a statistically significant difference was only observed in cases of maximum force and stiffness in TBD-treated mice (Fig. 1E). The effects of chemotherapeutic agents on the bone microstructure were exacerbated when the treatment was extended for another month (seven injections in total; Supplementary Fig. S1). These results indicated that treatment with ERI induced trabecular bone loss to a level comparable with that induced by treatment with DOX or TBD. In contrast, under the current experimental settings, ERI exhibited a relatively minor impact on nutrition, as suggested by the comparable body weights of ERI- and VCL-treated mice.

3.2. Treatment with ERI promotes osteoclastic bone resorption

To gain insight into the mechanism underlying bone mass loss induced by ERI administration, we performed a histomorphometric analysis using lumbar vertebral sections. We used vertebrae for

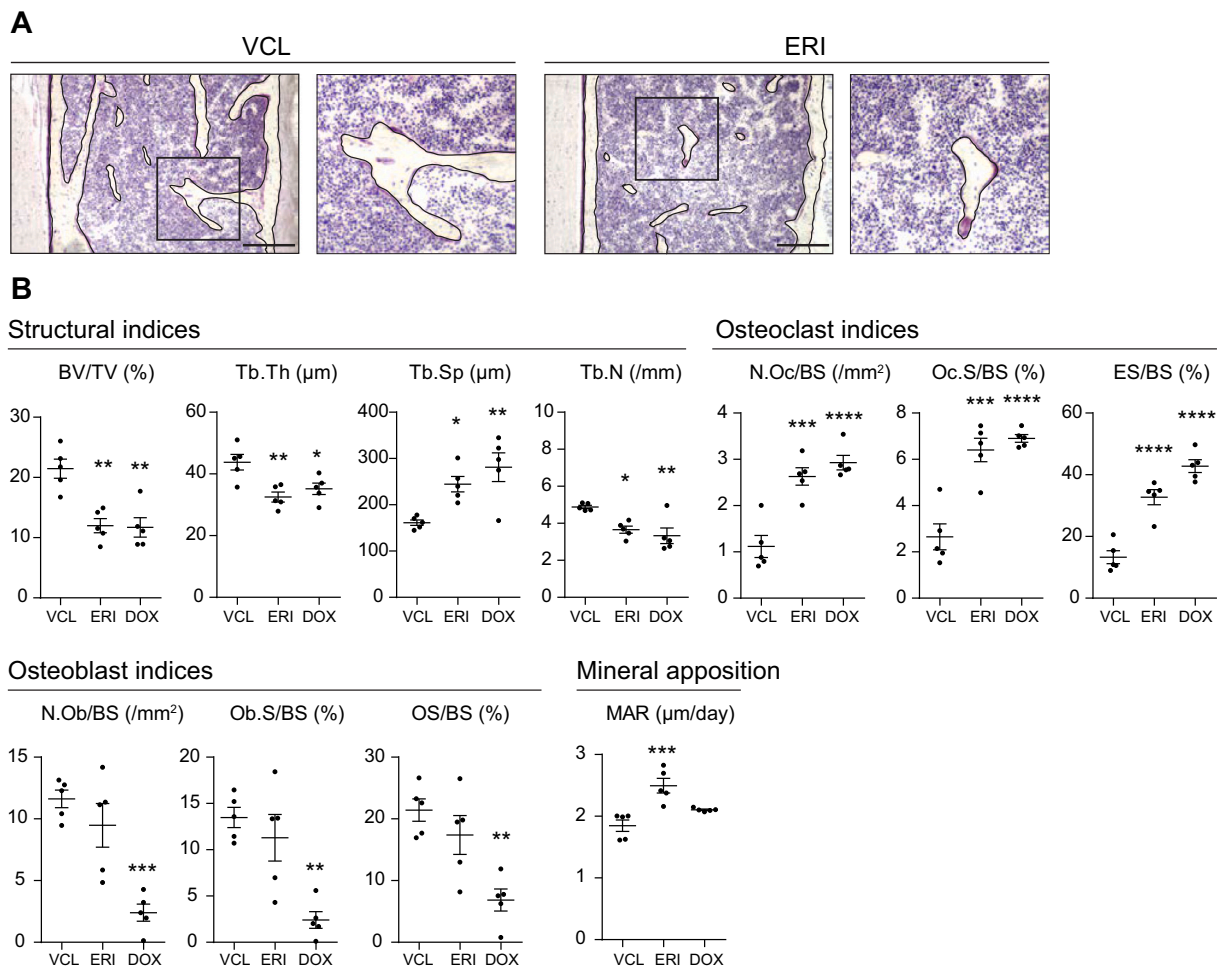


Fig. 2. Increased osteoclast activity in ERI-treated mice. A. Representative sections of the lumbar vertebrae collected from VCL- (left panels) and ERI- (right panels) treated mice. The right sections in each group show the high-magnification images of the boxed area in the left sections. The bone surface is artificially outlined by black lines for better visualization. Bars, 250 μ m. B. Structural indices, osteoclast indices, osteoblast indices, and MAR of VCL-, ERI-, and DOX-treated mice analyzed by histomorphometric analysis. Five mice per each treatment group were analyzed. *, $P < 0.05$; **, $P < 0.01$; ***, $P < 0.001$; ****, $P < 0.0001$ (compared with those in the VCL-treated group).

histomorphometric analysis because the number of trabeculae was significantly decreased in the tibiae in mice treated with chemotherapeutic agents and vertebrae are usually more abundant in trabeculae than tibiae. Mice treated with DOX, which has previously been shown to promote bone resorption and suppress bone formation (Yao et al., 2020), were also analyzed for comparison. Villanueva-stained sections showed a decrease in trabecular bone mass in ERI-treated mice compared with that in VCL-treated mice (Fig. 2A). In contrast, myelosuppression was not apparent in ERI-treated mice compared with that in VCL-treated mice as suggested by the comparable bone marrow cellularity between ERI-treated mice and VCL-treated mice.

The structural indices were nearly identical to the results of the μ CT analysis, except for Tb/Th, which was significantly lower in ERI- and DOX-treated mice than in VCL-treated mice (Fig. 2B). We also found a significant increase in osteoclast indices, including the number of osteoclasts per bone surface (N.Oc/BS), osteoclast surface per bone surface (Oc.S/BS), and erosion surface per bone surface (ES/BS) in both ERI- and DOX-treated mice compared with those in VCL-treated mice. Consistent with the results of a previous study (Yao et al., 2020), there was a significant decrease in osteoblast indices, including the number of osteoblasts per bone surface (N.Ob/BS), osteoblast surface per bone surface (Ob.S/BS), and osteoid surface per bone surface (OS/BS) in DOX-treated mice compared with those in VCL-treated mice. However, there were no statistically significant differences in any of the osteoblast indices between the ERI- and VCL-treated mice. Of note, there was an increase in mineral apposition in ERI-treated mice, as indicated by the increased mineral apposition rate (MAR) compared with those in VCL-treated mice. These results indicate that bone mass loss in ERI-treated mice was primarily caused by increased osteoclastic bone resorption, but not by suppression of osteoblast activity, and that mineral apposition was increased potentially through a coupling mechanism with increased

bone resorption. Accordingly, we found that ERI does not directly affect the differentiation of primary osteoblasts or mineralization *in vitro*, as evidenced by similar levels of Alizarin Red staining between VCL-treated and ERI-treated cells (Supplementary Fig. S2A).

3.3. ERI has no direct effect on osteoclast differentiation *in vitro*

Based on the results of the histomorphometric analysis, we investigated whether ERI directly affects osteoclastogenesis. We used RAW264.7, a macrophage/monocyte-like cell line that has the potential to differentiate into TRAP-positive multinucleated cells. Cells were incubated for six days in the presence of soluble RANK ligand and ERI and subsequently stained for TRAP. As shown in Fig. 3A and B, no apparent difference was observed in the number of TRAP-positive cells at any level of ERI exposure. Accordingly, ERI had no impact on the expression levels of transcripts that are induced during osteoclast differentiation, including *Nfatc1*, *Ctsk* (encoding cathepsin K), and *Acp5* (encoding TRAP) (Fig. 3C). We repeated the differentiation experiment with primary bone marrow cells and obtained essentially the same results (Fig. 3D).

3.4. Production of testosterone is not suppressed in ERI-treated mice

Because we did not observe any direct effect of ERI on osteoclastogenesis *in vitro*, we next investigated whether there were environmental changes that could lead to increased osteoclast activity in ERI-treated mice. Malnutrition and hypogonadism often occur in patients undergoing long-term chemotherapy and can lead to bone mass loss. Given that treatment with ERI did not result in significant body weight loss (Fig. 1A), it is unlikely that the ERI-treated mice suffered from severe malnutrition. Therefore, we examined the serum levels of testosterone, a

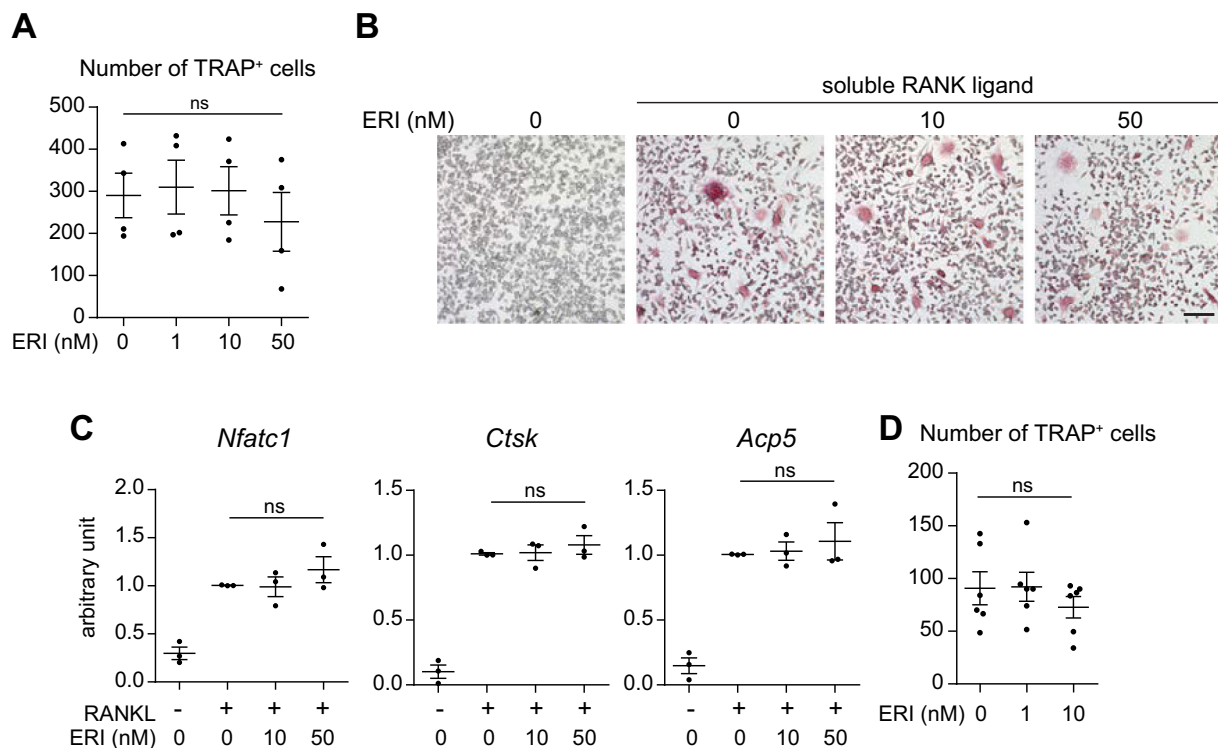


Fig. 3. ERI does not directly promote osteoclastogenesis *in vitro*. A and B. RAW264.7 cells were cultured with soluble RANK ligand in the presence of ERI (0, 1, 10, or 50 nM) for six days. Cells were stained for TRAP and the number of TRAP-positive multinucleated cells was counted. Representative photomicrographs of each treatment sample are shown in B. Bar, 100 μ m. C. RAW264.7 cells were cultured with/without soluble RANK ligand (RANKL) in the presence of ERI (10 or 50 nM) for 48 h. Cells were collected and the expression levels of *Nfatc1*, *Ctsk*, and *Acp5* transcripts were evaluated. Four independent experiments were performed. D. Primary bone marrow macrophages were cultured with soluble RANK ligand in the presence of ERI (0, 1, or 10 nM) for six days. Cells were stained for TRAP and the number of TRAP-positive multinucleated cells was counted. Six independent experiments were performed. ns, not significant.

gonadal hormone involved in the maintenance of bone mass. However, as shown in Fig. 4A, serum testosterone levels were comparable between VCL- and ERI-treated mice, indicating that ERI administration did not lead to hypogonadism under the present experimental conditions.

3.5. Expression of OPG transcripts is decreased in ERI-treated mice

Overt osteoclastic bone resorption observed in ERI-treated mice could be caused by increased expression of the RANK ligand, one of the most critical regulators of osteoclastogenesis that is expressed on osteoblasts and osteocytes. To test this hypothesis, we performed quantitative PCR using cDNA prepared from the femurs. While we found no increase in the expression level of *Tnfsf11* (encoding RANK ligand), there was a significant decrease in the expression level of *Tnfrsf11b* (encoding OPG, a soluble decoy receptor for RANK ligand) in ERI-treated mice compared with those in VCL-treated mice (Fig. 4B). Consequently, the *Tnfsf11/Tnfrsf11b* ratio was significantly increased in ERI-treated mice compared with that in VCL-treated mice, indicating a relative increase in the availability of RANK ligand in ERI-treated mice.

To further validate this finding, we examined whether there was a change in the osteoclast precursor pool in the bone marrow, which could be expanded by the RANK ligand (Fukasawa et al., 2016). Bone marrow cells were collected from VCL- and ERI-treated mice and analyzed using flow cytometry. As shown in Fig. 4C, there was a marked increase in the osteoclast precursor population (CD115⁺ CD117⁺ CD11^{dull} cells) (Arai et al., 1999). We performed the analysis using five mice for each treatment and confirmed a statistically significant increase in the ratio of osteoclast precursors in ERI-treated mice compared with that in VCL-treated mice (Fig. 4D). These results indicate that the relative increase in RANK ligand availability (owing to the decreased expression of OPG) leads to the expansion of the osteoclast precursor pool and increased osteoclast activity, ultimately leading to bone mass loss in ERI-treated mice.

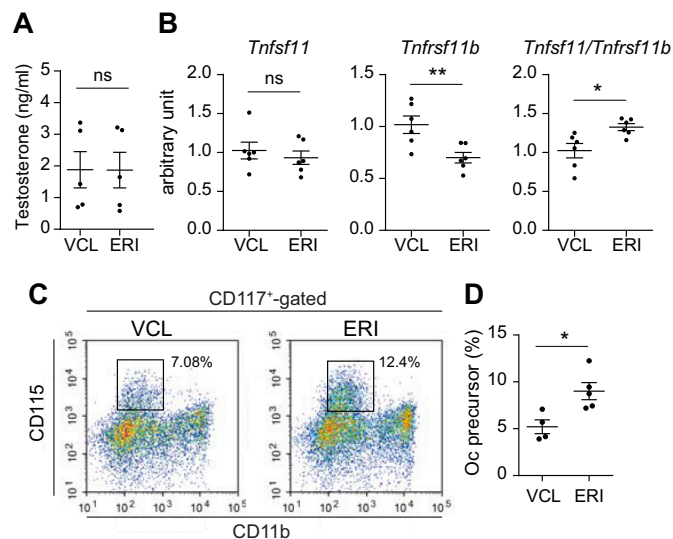


Fig. 4. The *Tnfsf11/Tnfrsf11b* ratio and the population of osteoclast precursors are increased in ERI-treated mice. A. Serum testosterone levels in VCL- and ERI-treated mice. Five mice per each treatment group were analyzed. B. Expression levels of *Tnfsf11* and *Tnfrsf11b* transcripts and the *Tnfsf11/Tnfrsf11b* ratio in the femurs collected from VCL- and ERI-treated mice. Six mice per each treatment group were analyzed. C. Flow cytometric analysis of the osteoclast precursors in the bone marrow cells collected from VCL- and ERI-treated mice. Boxed areas indicate the osteoclast precursors (CD115⁺ CD117⁺ CD11^{dull} cells). D. The ratio of osteoclast (Oc) precursors among CD115⁺-gated bone marrow cells. Five mice per each treatment group were analyzed. ns, not significant; *, $P < 0.05$; **, $P < 0.01$.

3.6. Administration of ZOL offsets the effects of ERI on bone mass

Our analysis suggests that the bone mass loss caused by ERI administration was mainly caused by overt bone resorption but not by decreased bone formation. This finding led to the hypothesis that the pharmaceutical inhibition of osteoclast activity could offset the effects of ERI on bone mass. To test this hypothesis, we used ZOL, a bisphosphonate with potent anti-osteoclast activity, and examined the effect of ZOL administration on bone microstructure and BMD in ERI-treated mice. Mice were randomly divided into four groups: VCL-, ERI-, ZOL-, and ERI + ZOL (E + Z)-treated. ERI was intravenously administered once a week for three weeks, and ZOL (100 $\mu\text{g}/\text{kg}$) was intraperitoneally injected concomitantly with the first administration of ERI. As shown in Fig. 5A and B, all the structural indices in the E + Z-treated mice were comparable with those in the ZOL-treated mice, indicating that a single administration of ZOL was sufficient to offset the bone mass loss caused by ERI treatment. Accordingly, we found that ZOL treatment fully recovered the trabecular BMD deficit in the ERI-treated mice to levels similar to those in mice solely treated with ZOL (Fig. 5C). These results further support the idea that bone mass loss in ERI-treated mice is predominantly caused by overt bone resorption and can be fully rescued by the inhibition of bone resorption.

4. Discussion

In this study, we aimed to elucidate the potential effects of ERI, a chemotherapeutic agent used to treat patients with breast cancer and liposarcomas (Cortes et al., 2011; Schoffski et al., 2016), on bone metabolism. We found that ERI induces bone mass loss by promoting osteoclastic bone resorption but not by suppressing osteoblastic bone formation. Mechanistically, we showed that ERI suppressed the expression of *Tnfrsf11b* transcripts, thereby increasing the *Tnfsf11/Tnfrsf11b* ratio, which could ultimately lead to an increase in osteoclast activity and the ratio of osteoclast precursors in the bone marrow. Consistent with these findings, our data showed that the administration of ZOL fully rescued bone mass loss induced by ERI in mice.

While most chemotherapeutic agents could potentially impair the function of gonadal glands and thereby lead to bone mass loss, recent studies have shown that chemotherapeutic agents induce bone mass loss independent of gonadal hormones. DOX, one of the most commonly used chemotherapeutic agents, has been shown to suppress osteoblast survival and differentiation through a signaling pathway mediated by oxidative stress and TGF- β (Rana et al., 2013). Furthermore, a recent study showed that DOX promoted bone mass loss by inducing cell senescence and a senescence-associated secretory phenotype (Yao et al., 2020). TBD suppresses bone formation by a direct inhibitory effect on osteoblasts and by suppressing macrophage efferocytosis (which in turn results in decreased TGF- β production) (Sinder et al., 2017). The results of our morphometric analyses indicated that bone mass loss induced by ERI was mainly due to increased osteoclast activity and that its potential effects on osteoblasts are negligible, at least under the present experimental conditions (Fig. 2B). This observation was in contrast to that in DOX-treated mice, where osteoclast activity increased and osteoblast activity was suppressed (Yao et al., 2020). The circumvention of bone loss after concomitant treatment with ZOL, which robustly inhibits osteoclastic bone resorption, and ERI supports these findings. Importantly, our data also showed that the effects of ERI on bone mass were not secondary to hypogonadism or malnutrition, as evidenced by the comparable body weights and serum testosterone levels between VCL- and ERI-treated mice (Figs. 1A and 4A). Although it is not yet fully clear how ERI regulates osteoclast activity and differentiation, our gene expression analyses suggest that a relative increase in RANK ligand availability, due to the decreased expression of its decoy receptor OPG, is at least in part involved in the overt osteoclast activity observed in ERI-treated mice. The finding of flow cytometry that the osteoclast precursor ratio was higher in ERI-treated mice than in VCL-treated mice

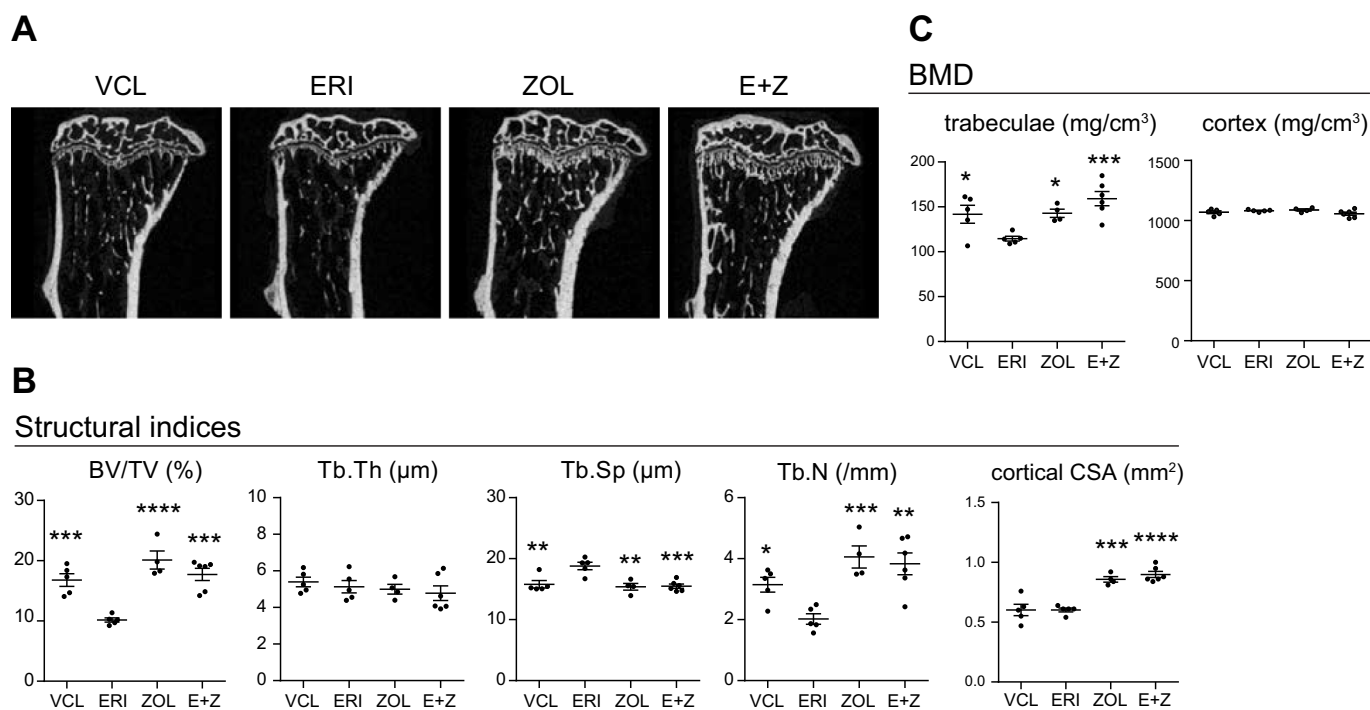


Fig. 5. ZOL offsets the bone mass loss induced by ERI. A. Representative reconstructed μ CT images of the proximal tibia of each treatment group. B and C. Structural indices (B) and BMD (C) of the mice in each treatment group. Five mice per each treatment group were analyzed. *, $P < 0.05$; **, $P < 0.01$; ***, $P < 0.001$; ****, $P < 0.0001$ (compared with those in the ERI-treated group).

may also support this contention.

According to the dose conversion formula (Nair and Jacob, 2016), the doses of each agent in mice used in the present study are equivalent to 15 mg/m² (DOX), 0.3 mg/m² (TBD), and 3 mg/m² (ERI) in humans (reference body weight 60 kg and body surface area 1.62 m²). The recommended administration doses of each agent are 60–75 mg/m² (21-day cycle), 1.5 mg/m² (21-day cycle), and 1.4 mg/m² (on Days 1 and 8, 21-day cycle) for DOX, TBD, and ERI, respectively. Because each agent was administered three times in the present study, the total amounts of each agent given to each mouse were 45 mg/m² (DOX), 0.9 mg/m² (TBD), and 9 mg/m² (ERI). Therefore, the total doses of each agent administered to mice can be assumed to be not significantly different from the total dose administered during one chemotherapy cycle in humans and within the clinically relevant range. Nevertheless, considering the biological differences between humans and mice that may affect the pharmacodynamics of these agents, the results of the present study and their relevance to humans need to be cautiously interpreted.

This study has several limitations. First, and most critically, as discussed above, there are intrinsic and unavoidable issues in using mice as an experimental model to evaluate the potential pharmaceutical effects of chemotherapeutic agents in humans. Nevertheless, our data clearly illustrate the effect of ERI on osteoclasts and how this effect can be fully suppressed by bisphosphonate administration. Therefore, although our results need to be further examined to determine if they can be translated into humans, they provide important clues as to how ERI affects bone metabolism in humans. Second, while our data indicate that osteoclastic bone resorption is induced by the administration of ERI through the downregulation of OPG, the underlying mechanism that links ERI and the transcriptional regulation of *Tnfrsf11b* remains to be elucidated. We performed experiments using primary osteoblasts to examine whether ERI directly regulates *Tnfrsf11b* expression in osteoblasts; however, we could not reproduce the effect of ERI observed *in vivo* (Supplementary Fig. S2B). Furthermore, the possibility that ERI can regulate osteoclast activity through different mechanisms independent of OPG cannot be ruled out.

In conclusion, the present study underscores the notion that chemotherapeutic agents can affect bone mass independent of their effects on gonadal glands and nutrition and reveals that ERI induces bone mass loss by promoting osteoclastic bone resorption, at least in part, by downregulating the transcription of *Tnfrsf11b*. The finding that ZOL offsets the effect of ERI on bone mass may also have important clinical implications as this further strengthens the idea that the risk of developing CTIBL in cancer survivors can be effectively reduced with proper interventions.

CRedit authorship contribution statement

Takahiro Ishizaka: Conceptualization, Formal analysis, Investigation, Writing – review & editing. **Keisuke Horiuchi:** Conceptualization, Data curation, Formal analysis, Funding acquisition, Supervision, Writing – original draft, Writing – review & editing. **Shinya Kondo:** Investigation, Writing – review & editing. **Masashi Isaji:** Investigation, Writing – review & editing. **Takahiro Nakagawa:** Investigation, Writing – review & editing. **Masahiro Inoue:** Investigation, Writing – review & editing. **Hajime Rikitake:** Investigation, Writing – review & editing. **Eiko Taguchi:** Investigation, Writing – review & editing. **Michiro Susa:** Conceptualization, Writing – review & editing. **Masaki Yoda:** Investigation, Writing – review & editing. **Takeshi Ono:** Investigation, Writing – review & editing. **Yusuke Kozai:** Data curation, Writing – review & editing. **Kazuhiro Chiba:** Funding acquisition, Supervision, Writing – review & editing.

Declaration of competing interest

All authors declare that they have no conflicts of interests.

Data availability

Data will be made available on request.

Acknowledgments

The authors thank Takemi Oguma (Department of Orthopedic Surgery, National Defense Medical College), Hiroshi Haraga, and Nobuyuki Tani-Ishii (Department of Oral Interdisciplinary Medicine, Kanagawa Dental University Graduate School of Dentistry) for their technical assistance. The study was in part supported by the grant from the Japan Society for the Promotion of Science (9K09613).

Appendix A. Supplementary data

Supplementary data to this article can be found online at <https://doi.org/10.1016/j.bonr.2023.101693>.

References

- Amend, S.R., Valkenburg, K.C., Pienta, K.J., 2016. Murine hind limb long bone dissection and bone marrow isolation. *J. Vis. Exp.* 110.
- Arai, F., Miyamoto, T., Ohneda, O., Inada, T., Sudo, T., Brasel, K., Miyata, T., Anderson, D.M., Suda, T., 1999. Commitment and differentiation of osteoclast precursor cells by the sequential expression of c-Fms and receptor activator of nuclear factor kappaB (RANK) receptors. *J. Exp. Med.* 190 (12), 1741–1754.
- Chai, R.C., McDonald, M.M., Terry, R.L., Kovacic, N., Down, J.M., Pettitt, J.A., Mohanty, S.T., Shah, S., Haffari, G., Xu, J., Gillespie, M.T., Rogers, M.J., Price, J.T., Croucher, P.L., Quinn, J.M.W., 2017. Melphalan modifies the bone microenvironment by enhancing osteoclast formation. *Oncotarget* 8 (40), 68047–68058.
- Cortes, J., O'Shaughnessy, J., Loesch, D., Blum, J.L., Vahdat, L.T., Petrakova, K., Chollet, P., Manikas, A., Dieras, V., Delozier, T., Vladimirov, V., Cardoso, F., Koh, H., Bougnoux, P., Dutcus, C.E., Seegobin, S., Mir, D., Meneses, N., Wanders, J., Twelves, C., E. investigators, 2011. Eribulin monotherapy versus treatment of physician's choice in patients with metastatic breast cancer (EMBRACE): a phase 3 open-label randomised study. *Lancet* 377 (9769), 914–923.
- Couzin-Frankel, J., 2019. Beyond survival. *Science* 363 (6432), 1166–1169.
- Demetri, G.D., von Mehren, M., Jones, R.L., Hensley, M.L., Schuetz, S.M., Staddon, A., Milhem, M., Elias, A., Ganjoo, K., Tawbi, H., Van Tine, B.A., Spira, A., Dean, A., Khokhar, N.Z., Park, Y.C., Knoblauch, R.E., Parekh, T.V., Maki, R.G., Patel, S.R., 2016. Efficacy and safety of trabectedin or dacarbazine for metastatic liposarcoma or leiomyosarcoma after failure of conventional chemotherapy: results of a phase III randomized multicenter clinical trial. *J. Clin. Oncol.* 34 (8), 786–793.
- Dybdal-Hargreaves, N.F., Risinger, A.L., Mooberry, S.L., 2015. Eribulin mesylate: mechanism of action of a unique microtubule-targeting agent. *Clin. Cancer Res.* 21 (11), 2445–2452.
- Fan, C., Georgiou, K.R., Morris, H.A., McKinnon, R.A., Keefe, D.M.K., Howe, P.R., Xian, C.J., 2017. Combination breast cancer chemotherapy with doxorubicin and cyclophosphamide damages bone and bone marrow in a female rat model. *Breast Cancer Res. Treat.* 165 (1), 41–51.
- Fukasawa, K., Park, G., Iezaki, T., Horie, T., Kanayama, T., Ozaki, K., Onishi, Y., Takahata, Y., Yoneda, Y., Takarada, T., Kitajima, S., Vacher, J., Hinoi, E., 2016. ATF3 controls proliferation of osteoclast precursor and bone remodeling. *Sci. Rep.* 6, 30918.
- Georgiou, K.R., King, T.J., Scherer, M.A., Zhou, H., Foster, B.K., Xian, C.J., 2012. Attenuated Wnt/beta-catenin signalling mediates methotrexate chemotherapy-induced bone loss and marrow adiposity in rats. *Bone* 50 (6), 1223–1233.
- Guise, T.A., 2006. Bone loss and fracture risk associated with cancer therapy. *Oncologist* 11 (10), 1121–1131.
- Handforth, C., D'Oronzo, S., Coleman, R., Brown, J., 2018. Cancer treatment and bone health. *Calcif. Tissue Int.* 102 (2), 251–264.
- Huang, T.C., Chiu, P.R., Chang, W.T., Hsieh, B.S., Huang, Y.C., Cheng, H.L., Huang, L.W., Hu, Y.C., Chang, K.L., 2018. Epirubicin induces apoptosis in osteoblasts through death-receptor and mitochondrial pathways. *Apoptosis* 23 (3–4), 226–236.
- Inoue, M., Horiuchi, K., Susa, M., Taguchi, E., Ishizaka, T., Rikitake, H., Matsushashi, Y., Chiba, K., 2022. Trabectedin suppresses osteosarcoma pulmonary metastasis in a mouse tumor xenograft model. *J. Orthop. Res.* 40 (4), 945–953.
- Kanis, J.A., McCloskey, E.V., Powles, T., Paterson, A.H., Ashley, S., Spector, T., 1999. A high incidence of vertebral fracture in women with breast cancer. *Br. J. Cancer* 79 (7–8), 1179–1181.
- Kommalapati, A., Tella, S.H., Esquivel, M.A., Correa, R., 2017. Evaluation and management of skeletal disease in cancer care. *Crit. Rev. Oncol. Hematol.* 120, 217–226.
- Mougalian, S.S., Kish, J.K., Zhang, J., Liassou, D., Feinberg, B.A., 2021. Effectiveness of eribulin in metastatic breast cancer: 10 years of real-world clinical experience in the United States. *Adv. Ther.* 38 (5), 2213–2225.
- Nair, A.B., Jacob, S., 2016. A simple practice guide for dose conversion between animals and human. *J. Basic Clin. Pharm.* 7 (2), 27–31.
- Neo, J., Fettes, L., Gao, W., Higginson, I.J., Maddocks, M., 2017. Disability in activities of daily living among adults with cancer: a systematic review and meta-analysis. *Cancer Treat. Rev.* 61, 94–106.
- Rachner, T.D., Coleman, R., Hadji, P., Hofbauer, L.C., 2018. Bone health during endocrine therapy for cancer. *Lancet Diabetes Endocrinol.* 6 (11), 901–910.
- Rana, T., Chakrabarti, A., Freeman, M., Biswas, S., 2013. Doxorubicin-mediated bone loss in breast cancer bone metastases is driven by an interplay between oxidative stress and induction of TGFbeta. *PLoS One* 8 (10), e78043.
- Rees-Punia, E., Newton, C.C., Parsons, H.M., Leach, C.R., Diver, W.R., Grant, A.C., Masters, M., Patel, A.V., Teras, L.R., 2023. Fracture risk among older cancer survivors compared with older adults without a history of cancer. *JAMA Oncol.* 9 (1), 79–87.
- Saad, F., Adachi, J.D., Brown, J.P., Canning, L.A., Gelmon, K.A., Josse, R.G., Pritchard, K. I., 2008. Cancer treatment-induced bone loss in breast and prostate cancer. *J. Clin. Oncol.* 26 (33), 5465–5476.
- Schoffski, P., Chawla, S., Maki, R.G., Italiano, A., Gelderblom, H., Choy, E., Grignani, G., Camargo, V., Bauer, S., Rha, S.Y., Blay, J.Y., Hohenberger, P., D'Adamo, D., Guo, M., Chmielowski, B., Le Cesne, A., Demetri, G.D., Patel, S.R., 2016. Eribulin versus dacarbazine in previously treated patients with advanced liposarcoma or leiomyosarcoma: a randomised, open-label, multicentre, phase 3 trial. *Lancet* 387 (10028), 1629–1637.
- Shandala, T., Shen Ng, Y., Hopwood, B., Yip, Y.C., Foster, B.K., Xian, C.J., 2012. The role of osteocyte apoptosis in cancer chemotherapy-induced bone loss. *J. Cell. Physiol.* 227 (7), 2889–2897.
- Sinder, B.P., Zweifler, L., Koh, A.J., Michalski, M.N., Hofbauer, L.C., Aguirre, J.I., Roca, H., McCauley, L.K., 2017. Bone mass is compromised by the chemotherapeutic trabectedin in association with effects on osteoblasts and macrophage ferrocytosis. *J. Bone Miner. Res.* 32 (10), 2116–2127.
- Swami, U., Chaudhary, I., Ghalib, M.H., Goel, S., 2012. Eribulin — a review of preclinical and clinical studies. *Crit. Rev. Oncol. Hematol.* 81 (2), 163–184.
- Taguchi, E., Horiuchi, K., Senoo, A., Susa, M., Inoue, M., Ishizaka, T., Rikitake, H., Matsushashi, Y., Chiba, K., 2021. Eribulin induces tumor vascular remodeling through intussusceptive angiogenesis in a sarcoma xenograft model. *Biochem. Biophys. Res. Commun.* 570, 89–95.
- Xing, L., Schwarz, E.M., Boyce, B.F., 2005. Osteoclast precursors, RANKL/RANK, and immunology. *Immunol. Rev.* 208, 19–29.
- Yao, Z., Murali, B., Ren, Q., Luo, X., Faget, D.V., Cole, T., Ricci, B., Thotala, D., Monahan, J., van Deursen, J.M., Baker, D., Faccio, R., Schwarz, J.K., Stewart, S.A., 2020. Therapy-induced senescence drives bone loss. *Cancer Res.* 80 (5), 1171–1182.